Saudi Pharmaceutical Journal 27 (2019) 981–989

Contents lists available at ScienceDirect

Saudi Pharmaceutical Journal

journal homepage: www.sciencedirect.com

Original article

The influence of variations of furanosesquiterpenoids content of commercial samples of *myrrh* on their biological properties

Ali S. Alqahtani [a,b,*], Omar M. Noman [b], Md. Tabish Rehman [a], Nasir A. Siddiqui [a], Mohamed F. Alajmi [a], Fahd A. Nasr [b], Abdelaaty A. Shahat [a,b,c], Perwez Alam [a,*]

[a] Department of Pharmacognosy, College of Pharmacy, King Saud University, Riyadh, Saudi Arabia
[b] Medicinal, Aromatic and Poisonous Plants Research Center, College of Pharmacy, King Saud University, Riyadh, Saudi Arabia
[c] Chemistry of Medicinal Plants Dept., National Research Centre, 33 El Bohouth St. (former El Tahrirst.), Dokki, P. O. 12622, Giza, Egypt

ARTICLE INFO

Article history:
Received 21 May 2019
Accepted 24 July 2019
Available online 25 July 2019

Keywords:
Myrrh
Furanosesquiterpenoids
Cytotoxicity
Antioxidant
HPTLC
Molecular docking

ABSTRACT

Myrrh is an oleo-gum-resin produced in the stem of *Commiphora myrrha* (Burseraceae) and used for centuries for different medicinal purposes. The present work was designed to evaluate the cytotoxic and antioxidant properties of seventeen myrrh samples (S1–S17) obtained from different retail markets of Saudi Arabia and Yemen regions, along with two furanosesquiterpenoids (CM-1 and CM-2). The cytotoxicity assay was carried out on HepG2, MCF-7 and HUVEC cell lines. S2, S5, S10, S12, CM-1, CM-2 exhibited significant cytotoxicity against HepG2/MCF-7 cell lines [IC50 (μg/mL): 13.8/10, 14/10, 14.5/11.3, 18/13.2, 9.5/12.5, 10/15.8, respectively) compare to vinblastin (IC_{50} (μg/mL): 2/2.5) whereas the remaining samples were found as mild active or inactive. The antioxidant properties of the samples were tested by β-carotene-bleaching and DPPH free radical scavenging methods where the samples S8 (1000 μg/mL) exhibited the highest β-carotene bleaching (76.2%) and free radical scavenging activity (79.8%). The HPTLC analysis was performed on NP-HPTLC plate using toluene, chloroform and glacial acetic acid as mobile phase in ratio of 7:2.9:0.1 (V/V/V). The validated HPTLC method furnished sharp, intense and compact peaks of CM-1 and CM-2 at Rf = 0.39 and 0.44, respectively. The highest/lowest content of CM-1 and CM-2 were found in S12/S5 and S5/S17, respectively. The molecular docking studies of CM-1 and CM-2 with human DNA topoisomerase IIα have shown that both the compounds were bound the active sites of the respective enzymes. Molecular dynamics simulation studies further confirmed that the interactions of CM-1 and CM-2 with topoisomerase were stable in nature. This study will help us in selection of appropriate myrrh sample for the greater benefits of the population in the Middle East region.

1. Introduction

Commiphora myrrha (Burseraceae) is a small tree or a large shrub, grows in small sandy and rocky regions of Somalia, Sudan, Ethiopia, Kenya and Saudi Arabia (Baser et al., 2003). Myrrh (a reddish brown oleo-gum-resin) found in the stem of several *Commiphora* species including *C. myrrha* has been used since several centuries in the treatment of different medical complications like inflammations of oral and pharyngeal mucosa (Francis et al., 2004) and intestinal infections (El Ashry et al., 2003). Thorough literature work revealed the different pharmacological properties exhibited by myrrh, such as cytotoxicity (Al-Harbi et al., 1994), anti-inflammatory (Massoud et al., 2001), antibacterial (Saadabi et al., 2006) and antigastric ulcer (Al-Harbi et al., 1997) properties. The phytochemical investigations of myrrh started around a century ago, and hundreds of phytochemicals have been identified (Ahamad et al., 2007). The myrrh's Gum-resin-volatile oil are the major useful contents, where it contains (30–60%) gum including acidic polysaccharides, resin (25–40%), volatile oil (3–8%), eugenol, heerabolene and many furansesquiterpenes (Chevallier, 1996).

The secondary metabolite production is the manifestation of integrated impact of numerous ecological factors on the plant throughout their growth phases besides genetic factors. Few metabolites are simply produced under explicit environments, or

* Corresponding authors at: Department of Pharmacognosy, College of Pharmacy, King Saud University, Riyadh, Saudi Arabia (A.S. Alqahtani).
E-mail addresses: alalqahtani@ksu.edu.sa (A.S. Alqahtani), aperwez@ksu.edu.sa (P. Alam).
Peer review under responsibility of King Saud University.

Production and hosting by Elsevier

https://doi.org/10.1016/j.jsps.2019.07.007
1319-0164/

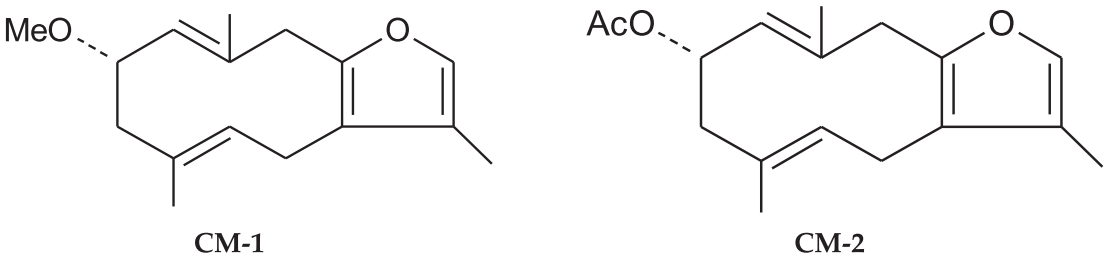

CM-1 CM-2

Fig. 1. Chemical structures of furanosesquiterpenoids (CM-1 and CM-2).

their amounts considerably increase underneath specific environments (Penuelas and Llusia, 1997). The chemical interface between plant and environmental conditions is interceded primarily by the secondary metabolite biosynthesis, which exercise its biological task, as an artificial adaptive retort to its environment. For that reason, the study of different variations is valuable in chemical characterization of plants (belonging to same species) collected from different regions (Stashenko et al., 2010; Lukas et al., 2009). Till now, no report has been published on the impact of variation of secondary metabolite content present in myrrh widely available in the Middle East region on its cytotoxic and antioxidant properties. Therefore, the present work was designed to evaluate the impact of content variation of two furanosesquiterpenoids (CM-1 and CM-2; Fig. 1) in seventeen myrrh samples collected from different regions (by validated HPTLC method) on their cytotoxic and antioxidant properties.

2. Experimental

2.1. Collection and processing of plant material

The seventeen samples (S1–S17) of myrrh (an oleo-gum-resin) were collected from different regions of gulf countries and they were assigned with different markings depending on the area of collection (Table 1).

Table 1
Sample codes and collection sites of different myrrh specimens.

Sample No.	Location	Place of purchase	Date of purchase
S1	Sana'a, Yemen	Bon Alyaman Spices	June 2017
S2		Sana'a Spices	June 2017
S3		Al-Arabiya Spices	August 2017
S4		Bn-Khaldon Spices	August 2017
S5		Socatra Spices	June 2017
S6	Al-Baha, Saudi	Banda Hypermarket	September 2018
S7	Arabia	Al-zahrani Spices	September 2018
S8	Riyadh, Saudi Arabia	Alothim Market	June 2016
S9		Banda Hypermarket	June 2016
S10		Aletkhan Spices	August 2016
S11		Alhomikani Spices	August 2016
S12		A'ali alkef Spices	September 2016
S13		Almarwani Spices	September 2016
S14		Bin Shalan Spices	October 2016
S15		Almanar Spices	October 2016
S16		Nora Spices	November 2016
S17			November 2016

2.2. Sample preparation, extraction and compounds isolation

2.2.1. Preparation of crude extract of S1–S17

The air dried sample (500 g) was coarsely powdered and extracted with 1000 mL ethanol (95%) for 3 days using cold maceration. The obtained ethanol extract was filtered and evaporated using a rotary evaporator and freeze dryer to give a dried ethanol extract (15 g). The ethanol extract was then suspended in distilled water and successively partitioned with n-hexane, chloroform ($CHCl_3$) and n-butanol (BuOH) to yield hexane (2 g), $CHCl_3$ (8 g) and BuOH (5 g) fractions, respectively.

2.2.2. Isolation of CM-1 and CM-2

Chloroform fraction (5 g) was chromatographed on a silica gel column (72 g; 80 × 3 cm). Elution started with 3% ethyl acetate in hexane and polarity was increased with ethyl acetate. The collected fractions (20 mL, each) were pooled depending on their TLC behavior to give 8 (A-H) fractions. Fraction C (70 mg), eluted with 5% ethyl acetate in hexane was rechromatographed on a silica gel column (7.2 g; 60 × 1 cm) and eluted gradually with 10% $CHCl_3$ in hexane. The collected fractions were merged into seven sub-fractions according to their TLC. Sub-fraction 4, eluted with 20% $CHCl_3$ in hexane yielded two known compounds CM-1 and CM-2. The structures of these compounds has been established by using ^{1}HNMR, 2D-NMR, IR and Mass spectroscopy and validated by the published data (Asafu, 1982).

Table 2
Cytotoxicity in terms of IC_{50} value (μg/mL) of different myrrh extracts (S1–S17).

Sample name	HepG2	MCF-7	HUVEC
S1	33.6 ± 0.6	71.3 ± 2.5	40.5 ± 1.9
S2	14.0 ± 0.9	9.8 ± 0.4	46.5 ± 1.0
S3	36.5 ± 1.6	68.8 ± 2.4	36.3 ± 2.0
S4	36.5 ± 0.8	31.3 ± 1.6	65.0 ± 2.4
S5	13.8 ± 0.2	9.5 ± 0.69	47.0 ± 0.9
S6	38.8 ± 1.1	33.2 ± 2.0	50.4 ± 1.7
S7	24.0 ± 0.9	26.0 ± 0.4	46.5 ± 1.0
S8	29.2 ± 0.5	20.7 ± 0.4	88.0 ± 2.0
S9	38.0 ± 0.5	47.9 ± 1.0	77.3 ± 1.5
S10	14.5 ± 0.5	11.3 ± 0.7	66.5 ± 1.8
S11	28.3 ± 0.6	23.5 ± 0.9	35.2 ± 1.0
S12	18.0 ± 0.5	13.2 ± 0.4	72.3 ± 1.4
S13	42.0 ± 0.9	32.2 ± 0.3	79.0 ± 1.5
S14	33.6 ± 0.6	71.3 ± 2.5	40.5 ± 1.9
S15	33.8 ± 0.6	33.0 ± 0.6	84.7 ± 0.8
S16	24.5 ± 0.7	21.3 ± 0.5	59.7 ± 1.3
S17	33.4 ± 0.8	35.5 ± 0.7	63.0 ± 2.0
CM-1	9.5 ± 0.5	12.5 ± 0.6	20.2 ± 0.8
CM-2	10.0 ± 0.4	15.8 ± 0.6	28.6 ± 0.8
Vinblastine	2.0 ± 0.3	2.5 ± 0.4	5.0 ± 0.4

2.3. Development of HPTLC method for analysis of CM-1 and CM-2 in S1-S17

CM-1 and CM-2 were isolated from chloroform fraction of ethanol extract of myrrh. The estimation of CM-1 and CM-2 in all samples of myrrh extracts (S1-S17) was carried out on 20 × 10 cm NP-HPTLC plate (Merck, Germany). Stock solution of standards CM-1 and CM-2 (1 mg/mL) were prepared in methanol and diluted further with methanol to get seven different dilutions ranging from 10 to 70 μg/mL. All the seven dilutions of CM-1 and

Table 3
β-Carotene-linoleic acid assay and DPPH free radical scavenging activities myrrh extracts (S1–S17).

Sample codes	β-carotene-linoleic acid test (% inhibition)	DPPH-radical scavenging activity (% inhibition)				
	1000 μg/mL	10 μg/mL	50 μg/mL	100 μg/mL	500 μg/mL	1000 μg/mL
S1	69.1 ± 0.9	31.9 ± 3.2	40.2 ± 2.1	50.4 ± 1.4	63.6 ± 2.4	71.2 ± 1.7
S2	45.8 ± 1.3	17.8 ± 0.8	24.5 ± 1.7	34.3 ± 0.9	44.3 ± 1.7	58.9 ± 2.6
S3	74.2 ± 2.0	30.2 ± 0.6	40.2 ± 1.3	51.3 ± 2.4	65.8 ± 2.0	76.5 ± 1.7
S4	70.1 ± 2.2	23.2 ± 1.2	30.1 ± 1.3	42.9 ± 0.7	56.8 ± 1.6	72.1 ± 1.2
S5	51.5 ± 1.9	2.4 ± 3.4	10.4 ± 4.3	21.6 ± 3.6	35.9 ± 3.5	54.4 ± 2.7
S6	68.2 ± 3.2	26.2 ± 2.5	32.7 ± 3.1	42.3 ± 2.1	59.2 ± 1.4	73.4 ± 0.7
S7	68.3 ± 1.5	27.3 ± 2.6	36.3 ± 1.4	47.1 ± 3.7	65.7 ± 2.1	74.4 ± 1.6
S8	76.2 ± 1.7	21.2 ± 3.1	37.1 ± 0.5	51.9 ± 3.2	70.6 ± 3.3	79.8 ± 2.8
S9	73.1 ± 1.2	29.2 ± 1.2	35.4 ± 1.5	44.8 ± 2.1	56.1 ± 2.3	75.4 ± 1.5
S10	57.2 ± 2.8	3.9 ± 0.8	11.5 ± 1.2	25.7 ± 1.4	40.8 ± 2.1	61.4 ± 1.3
S11	56.1 ± 2.3	4.8 ± 4.2	18.3 ± 3.1	37.1 ± 3.7	53.9 ± 2.8	62.4 ± 2.4
S12	65.2 ± 1.0	21.3 ± 0.4	27.8 ± 3.1	38.9 ± 1.1	50.9 ± 2.3	69.5 ± 1.2
S13	73.2 ± 2.7	11.4 ± 1.9	23.4 ± 0.4	43.1 ± 1.2	61.8 ± 2.7	76.7 ± 2.8
S14	44.2 ± 2.1	2.9 ± 4.3	17.4 ± 3.6	20.8 ± 1.3	33.2 ± 2.8	49.6 ± 3.7
S15	58.2 ± 1.6	7.4 ± 2.4	18.4 ± 1.8	24.2 ± 2.8	39.9 ± 1.5	61.4 ± 2.3
S16	41.2 ± 2.3	9.1 ± 4.1	14.2 ± 2.3	26.1 ± 3.1	31.2 ± 2.2	47.4 ± 2.1
S17	44.2 ± 3.1	10.3 ± 3.1	10.6 ± 3.1	21.6 ± 2.7	29.6 ± 3.1	44.7 ± 3.1
Ascorbic acid	NT	80.7 ± 2.5	86.1 ± 1.3	91.6 ± 1.2	93.7 ± 1.7	94.7 ± 0.4
Rutin	89.3	NT	NT	NT	NT	NT

NT means not tested. In the columns, means ± SD with different letters notification are significant at ($P < 0.05$) ($n = 3$).

CM-2 as well as all seventeen sample extracts (10 μL, each) were applied on HPTLC plate through a micro liter syringe attached with Automatic TLC Sampler-4 (CAMAG, Switzerland) with band size of 6 mm wide, each at a speed of 160 nL/sec to furnish a linearity range of 100–700 ng/band. Post application the TLC plate was developed in 20 × 10 cm pre-saturated twin-trough glass chamber (Automatic Development Chamber-2, CAMAG, Switzerland) at controlled temperature (25 ± 2 °C) and controlled humidity (60 ± 5%). The developed HPTLC plate was derivatized with vanillin in sulphuric acid and dried to give clear and compact spots of standard as well as different constituents of extracts, and analyzed quantitatively at λ = 530 nm in absorbance mode. The proposed high performance thin layer chromatographic method was validated [limit of detection (LOD), limit of quantification (LOQ), precision, recovery as accuracy and robustness were assessed] according to the ICH guideline (2005).

2.4. Biochemical studies

2.4.1. Cytotoxic activity

In this study, two different human cancer cells (MCF-7, breast), (HepG2, liver) and one normal human umbilical vein endothelial cells (HUVECs) were used. The cells were maintained in the DMEM medium supplemented with 10% FBS and 1% penicillin-streptomycin. Cells were plated at approximately 1×10^5 cells per well in 24-well tissue culture plates in 1 mL of medium, and incubated at 37 °C at 5% CO_2. After 24 h, the cells were treated with various concentrations (10 μg/mL, 25 μg/mL, 50 μg/mL and 100 μg/mL) of all myrrh extracts (S1-S17) and isolated compounds for 48 h. Next, 100 μL of MTT (5 mg/mL) was added to each well and incubated for 24 h. After incubation, 1 mL of 0.01 N HCL/Isopropanol was added to the wells to solubilize the formazan and was on the shaker for 10 min. The absorbance of converted MTT was measured at λ = 490 nm with a microplate reader (Bio-Tek, USA). Vinblastine was used as a positive control while wells with untreated cells were considered as controls. For each extract tested, the IC_{50} (concentration of tested compound needed to inhibit cell growth by 50%) was generated from the dose-response curves.

2.4.2. Determination of the antioxidant activity of S1–S17

2.4.2.1. Scavenging activity of DPPH radical. For the determination of the free radical scavenging, DPPH (2, 2-diphenyl-1-picrylhydrazyl) was utilized. The assay was completed as depicted by Brand-Williams et al., (1995). This test estimates the free radical scavenging ability of the examined extracts. Various concentrations (10, 50, 100, 500 and 1000 μg/mL) of all the extracts were used. Briefly, to obtain a total volume of 1 mL of the test mixture, 500 μL of the extract was mixed with 375 μL methanol and added 125 μL of 0.04% DPPH ethanol solution. Ascorbic acid was utilized as positive control. After 30 min of incubation at room temperature in the dark, the reduction in absorbance was estimated at λ = 517 nm. The radical scavenging ability was determined from the equation:

$$\% \text{ of radical scavenging activity} = (\text{Abs control - Abs sample} \,/\, \text{Abs control}) \times 100$$

2.4.2.2. β-Carotene–linoleic acid assay. The antioxidant activity of all the extracts was assessed by utilizing the β-carotene bleaching assay reported by Velioglu et al., (1998) with modifications. To flasks containing 0.02 mL of linoleic acid and 0.2 mL of Tween-20, 1 mL of a β-carotene solution (0.2 mg/mL in chloroform) was added. The chloroform was evaporated under reduced pressure at 40 °C. Then residue solution was directly diluted with 100 mL of distilled water and blended for 1–2 min to make an emulsion. A solution prepared likewise but without β-carotene was utilized as a blank. A control containing 0.2 mL of 80% (v/v) methanol instead of extract was additionally made. A 5 mL of the emulsion was added to a tube containing 0.2 mL of the sample extract at 1 mg/mL. Rutin (1 mg/mL) was utilized as a positive control. After that an incubation of the tubes in a water bath at 40 °C for 2 h was carried out. At the end, the Absorbance for test and standard solutions was measured against the blank at 470 nm at 30 min intervals, with a UV–visible spectrophotometer (UV mini-1240, Shimadzu, Japan). The antioxidant activity was determined utilizing the formula:

$$\% \text{ antioxidant activity} = (\text{Abs0} - \text{Abst}) / (\text{Abs0}^\circ - \text{Abst}^\circ) \times 100$$

where Abs0 and Abs0° are the absorbance readings at zero time of incubation for samples and control, respectively. Abst and Abst° are the absorbance readings for samples and control, respectively, after incubation for 120 min.

2.4.3. Molecular docking and molecular dynamics simulation studies of CM-1 and CM-2

The interaction of CM-1 and CM-2 with the ATPase domains of human DNA topoisomerase IIα (PDB ID: 1ZXM; 1.87 Å) was

evaluated by performing molecular docking and molecular dynamics simulation using different modules of Schrodinger suite in Maestro (Schrödinger, LLC, NY, USA) as described previously [Rehman et al., 2019; AlAjmi et al., 2018 a,b]. Briefly, the structures of ligands (CM-1 and CM-2) were drawn in 2D sketcher and prepared for docking using LigPrep (Schrödinger, LLC, NY, USA). All the possible conformations of ligands were generated at pH 7.0 ± 2.0 using Epik (Schrödinger, LLC, NY, USA) and energy minimized using OPLS3e forcefield. Proteins were optimized for docking using Glide (Schrödinger, LLC, NY, USA) by removing non-essential water molecules, adding hydrogen atoms, generating any missing side chains and loops using Prime (Schrödinger, LLC, NY, USA) and removing any other heterogenous molecule except bound ligands. Grids were generated by selecting the centeroid of the ligand as the center of grid box. The size of grid box for ATPase domain of human DNA topoisomerase IIα was 72 × 72 × 72 Å respectively. Molecular docking was performed with standard precision (SP) mode in Glide (Schrödinger, LLC, NY, USA) keeping all the parameters at default values. Molecular dynamics simulation was performed using Desmond (Schrödinger, LLC, NY, USA) for 25 ns using NTP ensemble at 300 K temperature and 1 bar atmospheric pressure. An orthorhombic simulation box was generated in the system builder in such a way as the boundaries of the box were at least 10 Å away from the protein. TIP3P explicit solvent model was employed to solvate the simulation box and proper counterions were added to neutralize the system. Further, 150 mM NaCl was added to the simulation box to mimic the physiological conditions. Before the start of simulation, the whole system was energy-minimized using OPLS3e forcefield till it converges to 1 kcal/mol/Å.

2.5. Statistical analysis

Statistical differences between control and treatment values of two parameters were analyzed with student's *t*-test using excel Microsoft office. Data were expressed as mean ± S.D. and the difference were statistically significant at $P < 0.05$ compared to control. All statistical charts were conducted using origin Lab software (version 8, Massachusetts, USA) and excel Microsoft office.

3. Results and discussion

3.1. Concurrent analysis of CM-1 and CM-2 in S1-S17 by validated HPTLC method

The mobile phase for CM-1 and CM-2 analysis in S1–S17 by HPTLC was selected by testing several different compositions of a range of solvents. Out of these a combination of toluene, chloroform and glacial acetic acid in the ratio of 7:2.9:0.1, v/v/v was found as the most suitable mobile phase for the development and HPTLC analysis (quantitative analysis) of CM-1 and CM-2. An intense, sharp and compact peak of CM-1 and CM-2 were found at Rf = 0.39 ± 0.001 and 0.44 ± 0.001, respectively (Fig. 2A). This method was found to be able to separate the standards CM-1 and CM-2 from various components of samples S1-S17 (Fig. 2B). The identities of the bands were confirmed by overlaying the spectra of all the extracts with the spectra of CM-1 and CM-2 (Fig. 2C). The developed method was validated according to ICH guideline, 2005 to determine the LOD, LOQ, precision, accuracy and robust-

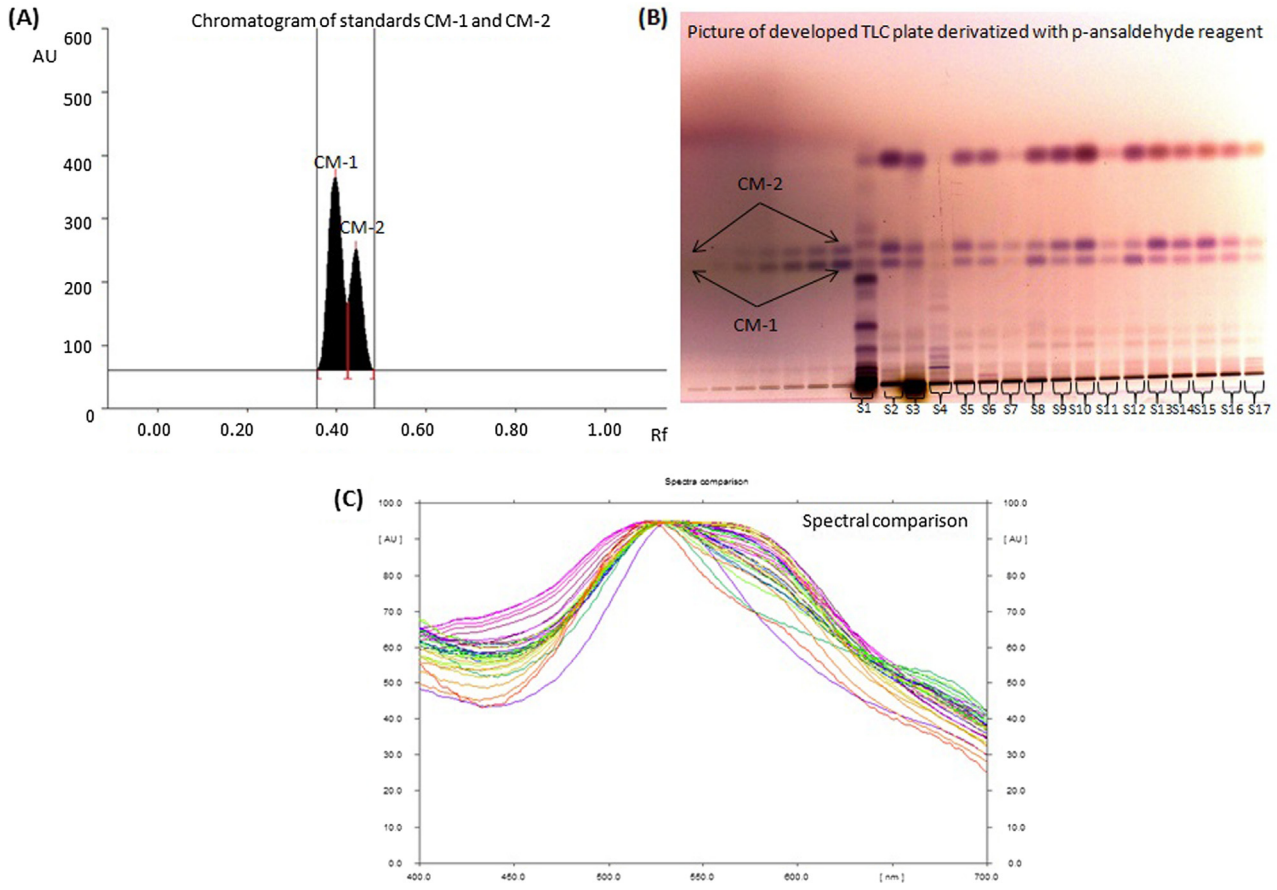

Fig. 2. Chromatogram of CM-1 and CM-2 in S1–S17 [mobile phase: toluene: chloroform: glacial acetic (7:2.9:0.1, v/v/v)]. (A) Chromatogram of standards CM-1 (Rf = 0.39 ± 0.001) and CM-2 (Rf = 0.44 ± 0.001) at λmax = 530 nm; (B) Pictogram of derivatized TLC plate in day light; (C) Spectral comparison of all tracks at 530 nm.

ness. It was found that the developed method was perfectly selective with good baseline resolution. The regression equation/correlation co-efficient (r^2) for CM-1 and CM-2 were found as Y = 2.183x + 780.563/0.9943 and Y = 1.001x + 36.465/0.9926, respectively in the linearity range 100–700 ng/spot. The LOD/LOQ (ng) for CM-1 and CM-2 were found as 31.53/95.57 and 25.24/76.49, respectively (Table 4). The recovery as accuracy study was recorded in Supplementary Table S1 for the proposed method. The recovery/ RSD (%) for CM-1 and CM-2 were found as 98.10–9 9.11/1.39–1.80 and 98.71–99.52/1.25–1.65, respectively. The intra-day and inter-day precision for the proposed method was recorded in Supplementary Table S2. The RSD (%) for intra-day/ inter-day precisions (n = 6) of CM-1 and CM-2 were found as 1.47–1.65/1.46–1.60 and 1.42–1.74/1.41–1.73, respectively, which illustrates good precision of the proposed method. A very small change was deliberately done (in mobile phase composition, saturation time and mobile phase volume) to check the robustness of the mobile phase and the data collected were reported in Supplementary Table S3. The low values of SD and % RSD indicated that the proposed method was robust.

The validated HPTLC method was applied to analyze CM-1 and CM-2 concurrently in all seventeen myrrh extracts (S1–S17). By using the above HPTLC method the quantity (μg/mg, of dried weight of extract) of CM-1 in all seventeen (S1–S17) extracts were found in the order of: S12(211.50) > S8(187.85) > S5(141.02) > S10 (136.33) > S6(133.06) > S2(131.01) > S9(107.08) > S13(101.05) > S11(91.87) > S16(82.53) > S14(78.54) > S7(50.91) > S17(49.36) > S4(18.65) > S1(15.89) > S3(15.61) > S15(9.32), while the content of CM-2 were found in the order of: S5(674.18) > S2(550.46) > S10(323.75) > S9(277.25) > S6(234.02) > S12(227.15) > S13 (203.04) > S7(192.95) > S4(175.70) > S8(132.47) > S15(130.25) > S11(125.12) > S14(122.41) > S16(94.60) > S1(37.32) > S3(35.03) > S17(23.61) (Table 5). It is evident from the obtained HPTLC data that the total content of both furanosesquiterpenoids (CM-1 and CM-2) were found in significant quantity in the S5 (Fig. 3A), S2 (Fig. 3B), S10 (Fig. 3C) and S12 (Fig. 3D).

3.2. Cytotoxic activity of S1–S17

In this study, all the seventeen myrrh extracts (S1–S17) were screened for their cytotoxic activities against two human cancer cell lines (Liver, HepG2), (Breast, MCF-7) and non-tumorigenic human umbilical vein endothelial cells (HUVECs) using MTT assay. The inhibition activity was assessed after 24 hrs following treatment. The results were expressed in terms of IC_{50} values which represent the concentration of the extract that was required to inhibit 50% of the cells and it was calculated from the dose-response curve (Table 2).

According to criteria of the American National Cancer Institute the IC_{50} value of a crude extract is considered a promising and active if it is lower than 20 μg/mL and moderately active if its IC_{50} ranges from 20 to 100 μg/mL (Skehan et al., 1990). Samples S2, S5, S10 and S12 showed IC_{50} values of less than 20 μg/ mL which can be considered as the promising sources of anticancer compounds (Table 2). Fractions S2 and S5 exhibited the highest activity against MCF-7 cells lines with IC_{50}, 9.8 and 9.5 μg/mL, respectively while fractions S2, S5, S10 and S12 showed strong cytotoxic property against HepG2 cells with IC_{50}, 13.8, 14.0, 14.5 and 18.0 μg/mL, respectively. In contrast, approximately all fractions exhibited moderate activity against non-tumorigenic HUVEC cells (Table 2). Accordingly, these fractions could be considered moderately active against normal cells. The isolated furanosesquiterpenoids CM-1 and CM-2 from the myrrh extract also exhibited strong cytotoxic property against HepG2/MCF-7 cell lines with IC_{50}: 9.5/12.5 and 10/15.8 μg/mL, respectively compared to standard drug vinblastin (IC_{50}: 2.0/2.5, μg/mL). The presence of CM-1 and CM-2 in significant quantities in myrrh samples S2, S5, S10 and S12 (evaluated by HPTLC method) also supported their excellent cytotoxic properties. Sesquiterpenes are a class of naturally occurring compounds found in plants and marines has demonstrated therapeutic potential in decreasing the progression of cancer (Modzelewska et al., 2005). A furano sesquiterpene isolated from soft coral (*Sinularia kavarittiensis*) was found to inhibit the proliferation of human cancer cell lines (THP-1) by cell membrane blebbing, chromatin condensation, DNA fragmentation, and decreasing pro-caspases 3, 9 level and increasing Bax/Bcl-2 ratio (Arepalli et al., 2009) while a sesquiterpenoid isolated from *S. lyratum* exhibited cytotoxic property against the MCF-7, HCT-8, A-549, SGC-7901 and BEL-7402 cell lines by inducing apoptosis, downregulating Bcl-2 expression and cleaving of (c)-caspase-3 and c-caspase-9 (Chen et al., 2017). These finding suggests that the sesquiterpenoids especially furanosesquiterpenes are very good cytotoxic agent and also supports our findings of strong cytotoxic property exhibited by some myrrh samples containing high amount of furanosesquiterpenoids CM-1 and CM-2.

3.3. Antioxidant activity of S1-S17

The results of the DPPH free radical scavenging and antioxidative activities (β-Carotene bleaching assay) of all the myrrh samples (S1–S17) are given in Table 3. In the *β*-carotene-bleaching model system all the samples showed variable resistance for the *β*-carotene bleaching at a concentration of 1000 μg/mL among which S3, S8, S9 and S13 exhibited good antioxidative property with 76.2, 74.2, 73.2 and 73.1% inhibition, respectively (Table 3). Moreover, results of the DPPH radical scavenging method demonstrated comparable free radical scavenging activity for all the

Table 4
R_f, Linear regression data for the calibration curve of CM-1 and CM-2 (n = 6).

Parameters	CM-1	CM-2
Linearity range (ng/spot)	100–700	100–700
Regression equation	Y = 2.183X + 780.563	Y = 1.001X + 36.465
Correlation (r^2) coefficient	0.9943	0.9926
Slope ± SD	2.183 ± 0.02	1.001 ± 0.007
Intercept ± SD	780.563 ± 28.73	36.465 ± 2.75
Standard error of slope	0.08	0.003
Standard error of intercept	11.72	1.12
R_f	0.39 ± 0.001	0.44 ± 0.001
LOD (ng)	31.53	25.24
LOQ (ng)	95.57	76.49

Table 5
HPTLC analysis of CM-1 and CM-2 in different myrrh extracts (S1–S17).

S. No.	Sample code	CM-1 content (μg/mg of dried weight of extract)	CM-2 content (μg/mg of dried weight of extract)
1.	S1	15.89 ± 0.75	37.32 ± 0.79
2	S2	131.01 ± 2.31	550.46 ± 3.91
3	S3	15.61 ± 0.38	35.03 ± 0.48
4	S4	18.65 ± 0.54	175.70 ± 1.89
5	S5	141.02 ± 2.55	674.18 ± 5.12
6	S6	133.06 ± 1.98	234.02 ± 2.32
7	S7	50.91 ± 1.84	192.95 ± 1.58
8	S8	187.85 ± 2.03	132.47 ± 1.96
9	S9	107.08 ± 1.73	277.25 ± 2.96
10	S10	136.33 ± 1.49	323.75 ± 2.30
11	S11	91.87 ± 0.88	125.12 ± 1.49
12	S12	211.50 ± 1.93	227.15 ± 1.13
13	S13	101.05 ± 2.01	203.04 ± 1.28
14	S14	78.54 ± 0.97	122.41 ± 1.14
15	S15	9.32 ± 0.22	130.25 ± 1.73
16	S16	82.53 ± 1.06	94.60 ± 1.18
17	S17	49.36 ± 1.53	23.61 ± 0.69

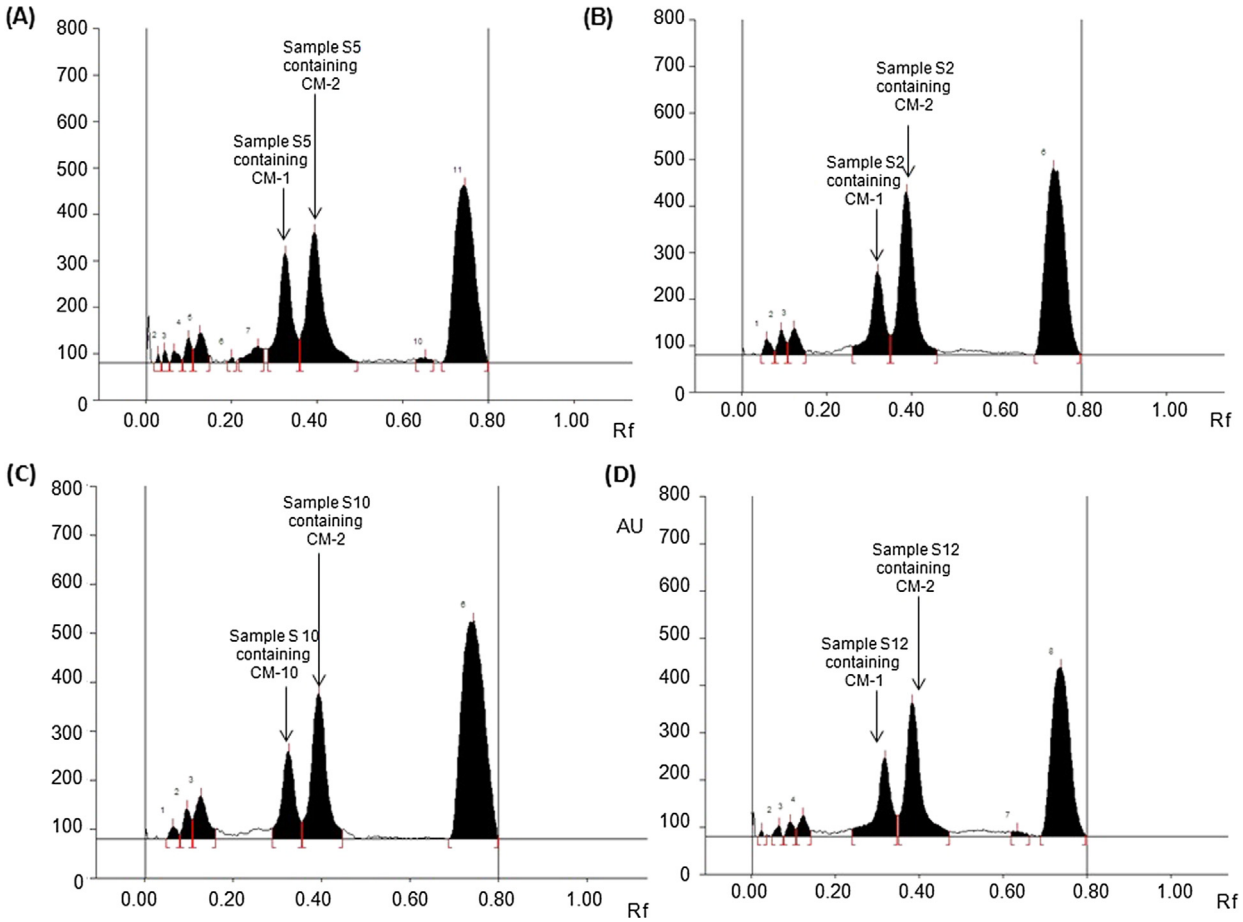

Fig. 3. Quantification of CM-1 and CM-2 in different myrrh samples (S1–S17) by HPTLC using toluene: chloroform: glacial acetic (7:2.9:0.1, v/v/v) as mobile phase. (A) Chromatogram of S5 [CM-1, spot 8, Rf = 0.39; CM-2, spot 9, Rf = 0.44)]; (B) Chromatogram of S2 [CM-1, spot 4, Rf = 0.39; CM-2, spot 5, Rf = 0.44)]; (C) Chromatogram of S10 [CM-1, spot 4, Rf = 0.39; CM-2, spot 5, Rf = 0.44)]; (D) Chromatogram of S12 [CM-1, spot 5, Rf = 0.39; CM-2, spot 6, Rf = 0.44)].

seventeen samples (Table 3). In addition to that, sample S8 exhibited the highest β-carotene bleaching and free radical scavenging activity among all the tested samples with 79.8% inhibition at the concentration of 1000 µg/mL. Both the isolated compounds CM-1 and CM-2 were found to be ineffective in controlling the free radicals as well as β-Carotene bleaching. Despite of the fact that CM-1 and CM-2 showed no antioxidant character but S3, S8, S9 and S13 exhibited excellent antioxidative effect which indicates the presence of several other phytoconstituents which were responsible for this property.

3.4. Molecular docking and molecular dynamics simulation analyses of CM-1 and CM-2

The docking protocol adopted in this study was validated by re-docking the ligand which was bound in the X-ray crystal structure of human DNA topoisomerase IIα. The docked and X-ray crystal poses of each ligands were superimposed and their root mean square deviations (RMSDs) were calculated. We found that the RMSDs of ligand bound to ATPase domain of human DNA topoisomerase IIα was found to be 0.5333 Å (Supplementary Figure S1A,B). The low values of RMSDs confirm that the dokcing procedure employed here was accurate.

3.4.1. Interaction of CM-1 and CM-2 with human DNA topoisomerase IIα

Human DNA topoisomerase IIα is a key enzyme in regulating the topology of DNA molecule during replication, transcription, recombination and repair. Thus, human DNA topoisomerase IIα is a good target for the development of new anticancer agents. In the present study, the ATPase domain of human DNA topoisomerase IIα has been selected to evaluate the binding efficacy of CM-1 and CM-2. Our results indicate that CM-1 as well as CM-2 binds strongly at the ATP binding site of human DNA topoisomerase IIα (Fig. 4). The human DNA topoisomerase IIα-CM-1 complex was stabilized by six hydrophobic interactions with Ile125, Pro126, Ile141, Phe142, Tyr165 and Ala167. Other amino acid residues that interact with CM-1 were Asn91, Asp94, Asn95, Arg98, Thr147, Ser148, Ser149, Asn150, Thr159, Gly161, Arg162, Asn163, Gly164, Tyr165, Gly166, Ala167, Lys168, and Gln376 (Fig. 4A and B). The docking energy and the corresponding docking affinity of CM-1 were estimated as -5.76 kcal mol^{-1} and 1.68×10^4 M^{-1} respectively (Table 6). Similarly, CM-2 and human DNA topoisomerase IIα complex was stabilized by two hydrogen bonds (Ser148 and Asn150) and four hydrophobic interactions with Ala92, Ile125, Ile141 and Phe142. Other residues involved in CM-2-human DNA topoisomerase IIα complex formation were Asn91, Asp94, Asn95, Arg98, Asn120, Lys123, Gly124, Thr127, Ser149, Gly161, Arg162, Gly164, Lys168, and Thr215 (Fig. 4C and D). In addition, Mg^{2+} also participated in stabilizing the complexes of CM-1 and CM-2 with human DNA topoisomerase IIα. The docking energy and the corresponding docking affinity of CM-2 were estimated as -6.12 kcal mol^{-1} and 3.08×10^4 M^{-1} respectively (Table 6). Further, the stability of human DNA topoisomerase IIα and CM-1/CM-2 complexes was evaluated by performing molecular dynamics simulation for 25 ns at 300 K. In Fig. 5, panels A and B

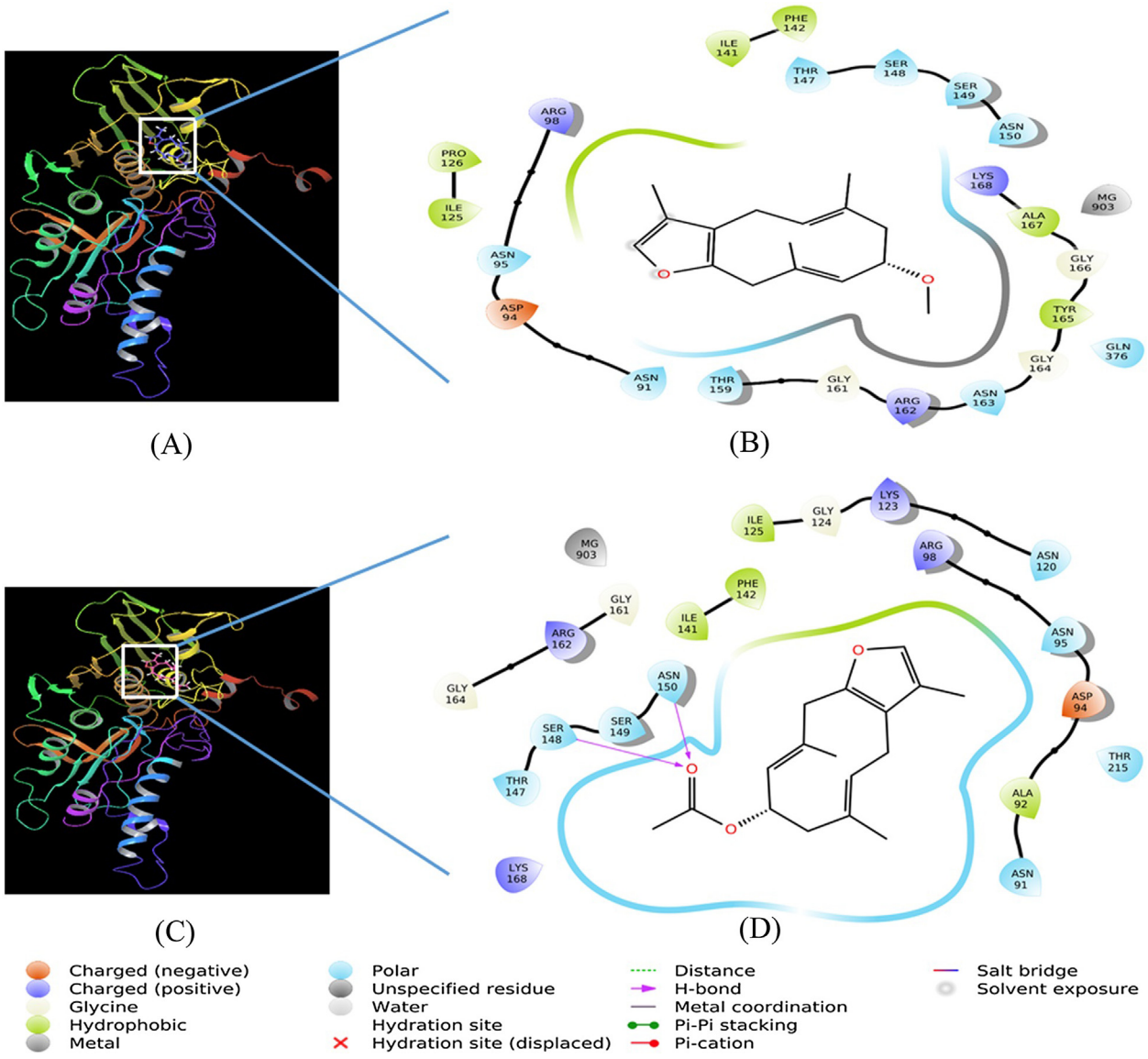

Fig. 4. Molecular docking of CM-1 (panel A) and CM-2 (panel B) with human DNA topoisomerase IIα.

Table 6
Molecular docking parameters for the interaction between ligands (CM-1 and CM-2) and protein (human DNA topoisomerase IIα).

Ligands	Hydrogen bonds	Hydrophobic interactions	Other residues	Docking energy (kcal mol^{-1})	Docking affinity (M^{-1})
Control Ligand (phosphoamino phosphonic acid-adenylate ester, ANP)	Glu87, Asn91, Asn120, **Ser148**, Arg162, Asn163, Gly166, Ala167, Gln376, Lys378	**Ala92**, **Ile125**, **Ile141**, **Phe142**, **Tyr165**, **Ala167**, Ile217	**Mg**[*], **Asn95**, **Arg98**, **Thr147**, **Ser149**, Asn150, Gly160, **Gly161**, **Gly164**, **Lys168**, **Thr215**, Lys378[#]	−13.03	3.60×10^9
CM-1	–	**Ile125**, Pro126, **Ile141**, **Phe142**, **Tyr165**, **Ala167**	**Mg**, Asn91, Asp94, **Asn95**, **Arg98**, **Thr147**, Ser148, **Ser149**, Asn150, Thr159, **Gly161**, **Arg162**, Asn163, **Gly164**, Tyr165, Gly166, Ala167, **Lys168**, Gln376	−5.76	1.68×10^4
CM-2	**Ser148**, Asn150	**Ala92**, **Ile125**, **Ile141**, **Phe142**	**Mg**, Asn91, Asp94, **Asn95**, **Arg98**, Asn120, Lys123, Gly124, Thr127, **Ser149**, **Gly161**, **Arg162 Gly164**, **Lys168**, **Thr215**	−6.12	3.08×10^4

Residues in bold are commonly involved in the interaction with ligands (control, CM-1 and CM-2).
[#] One salt bridge.
[*] Two salt bridges.

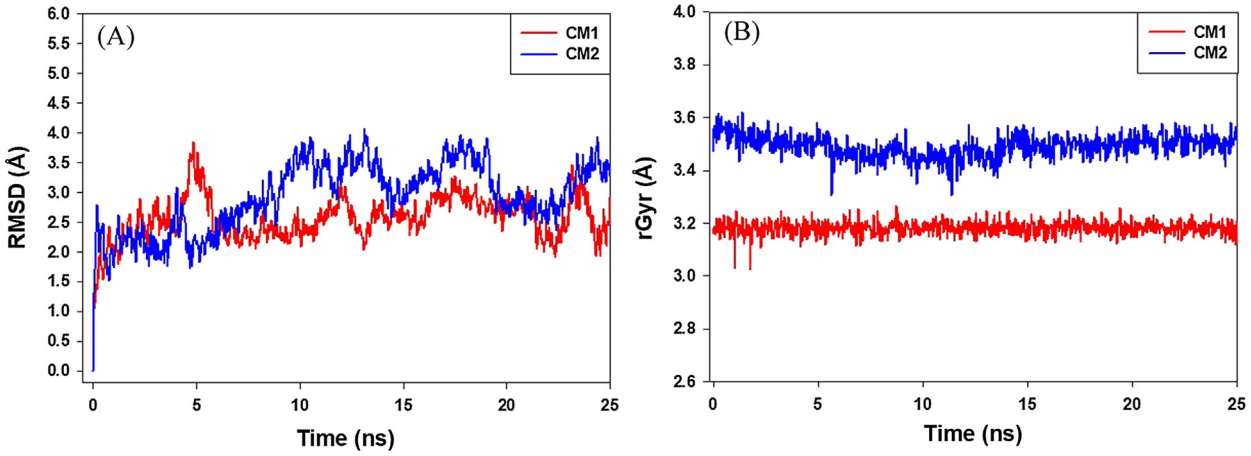

Fig. 5. Molecular dynamic (MD) simulation of CM-1 and CM-2 with proteins showing variation in root mean square deviations (RMSDs) and radius of gyration (rGyr) with simulation time. Panels A and B show RMSD and rGyr of human DNA topoisomerase IIα respectively.

respectively show the RMSD and radius of gyration (rGyr) of human DNA topoisomerase IIα with respect to the initial conformation in the presence of CM-1 and CM-2. It is evident that the RMSD values of human DNA topoisomerase IIα was stabilized after initial fluctuations and was within the upper limit of 2 Å (Fig. 5A). Also, rGyr of human DNA topoisomerase IIα did not deviate significantly from the initial structure, implying that the overall compactness of the protein remains unaltered during the course of simulation (Fig. 5B).

The molecular docking of control ligand (i.e. the inhibitor bound to protein in the X-ray structure, namely phosphoaminophosphonic acid-adenylate ester, ANP) with human DNA topoisomerase IIα revealed that it forms ten hydrogen bonds (Glu87, Asn91, Asn120, Ser148, Arg162, Asn163, Gly166, Ala167, Gln376, and Lys378) and seven hydrophobic interactions with Ala92, Ile125, Ile141, Phe142, Tyr165, Ala167, and Ile217. Moreover, Lys378 and Mg^{2+} formed one and two salt bridges respectively with the phosphate groups of ANP (Supplementary Figure S1C and D). The docking energy and the corresponding docking affinity of control ligand were estimated as -13.03 kcal mol^{-1} and 3.60×10^9 M^{-1} respectively (Table 6). It is interesting to note that most of the residues of human DNA topoisomerase IIα involved in the interaction with CM-1 and CM-2 were also engaged in the formation of human DNA topoisomerase IIα-ANP complex. These results corroborate well with the observed cytotoxic activities of CM-1 and CM-2. Molecular docking and simulation studies provided an insight into the probable mechanism behind the cytotoxic activities of CM-1 and CM-2 i.e. by binding to the ATPase domain and hence the inhibition of human DNA topoisomerase IIα.

4. Conclusion

The findings suggested that Myrrh samples (S2, S5, S10 and S12) along with two isolated compounds (CM-1 and CM-2) possess excellent cytotoxic potential which further verified by molecular docking and molecular dynamics simulation studies. The HPTLC analyses revealed a significant variation in their chemical contents (CM-1 and CM-2) which may be due to difference in climatic conditions in different regions of Yemen and Saudi Arabia. The quantitative analyses of CM-1 (S12) and CM-2 (S5) in all the samples of Myrrh facilitate the grading and selection of the effective one along with their estimation in herbal drugs and formulation by the proposed method. The overall outcome suggests the easiness of selection and use of Myrrh for cytotoxic and antioxidant potential.

Acknowledgement

The authors extend their appreciation to the Deanship of Scientific Research at King Saud University for funding this work through research group no. RG-262.

Declaration of Competing Interest

The authors report no declaration of interest. The authors alone are responsible for the content and writing of the paper.

Appendix A. Supplementary material

Supplementary data to this article can be found online at https://doi.org/10.1016/j.jsps.2019.07.007.

References

Ahamad, S.R., Al-Ghadeer, A.R., Ali, R., Qamar, W., Aljarboa, S., 2007. Analysis of inorganic and organic constituents of myrrh resin by GC–MS and ICP-MS: an emphasis on medicinal assets. Saudi Pharm. J. 25, 788–794.

Al-Harbi, M., Qureshi, S., Ahmed, M., Rafatullah, S., Shah, A., 1994. Effect of Commiphora molmol (oleo-gum-resin) on the cytological and biochemical changes induced by cyclophosphamide in mice. Am. J. Chin. Med. 22, 77–82.

AlAjmi, M.F., Alam, P., Rehman, M.T., Husain, M.F., Khan, A.A., Siddiqui, N.A., Hussain, A., Kalam, M.A., Parvez, M.K., 2018a. Interspecies anticancer and antimicrobial activities of genus *Solanum* and estimation of rutin by validated UPLC-PDA method. Evid. Based Complement. Altern. Med. 6040815, 1–13.

AlAjmi, M.F., Rehman, M.T., Hussain, A., Rather, G.M., 2018b. Pharmacoinformatics approach for the identification of Polo-like kinase-1 inhibitors from natural sources as anti-cancer agents. Int. J. Biol. Macromol. 116, 173–181.

Al-Harbi, M., Qureshi, S., Raza, M., Ahmed, M., Afzal, M., Shah, A.H., 1997. Gastric antiulcer and cytoprotective effect of *Commiphora molmol* in rats. J. Ethnopharmacol. 55, 141–150.

Arepalli, S.K., Sridhar, V., Venkateswara Rao, J., Kavin Kennady, P., Venkateswarlu, Y., 2009. Furano-sesquiterpene from soft coral, *Sinularia kavarittiensis*: induces apoptosis via the mitochondrial-mediated caspase-dependent pathway in THP-1, leukemia cell line. Apoptosis 14 (5), 729–740.

Asafu, M., 1982. Furanosesquiterpenoids of *C. erythraea* and *C. myrrh*. Phytochemistry 21 (3), 677–680.

Baser, K.H.C., Demirci, B., Dekebo, A., Dagne, E., 2003. Essential oils of some *Boswellia* spp., myrrh and opopanax. Flavour Frag. J. 18, 153–156.

Brand-Williams, W., Cuvelier, M.E., Berset, C., 1995. Use of a free radical method to evaluate antioxidant activity. LWT-Food Sci. Technol. 28, 25–30.

Chen, M., Wu, J., Zhang, X.X., Wang, Q., Yan, S.H., Wang, H.D., Liu, S.L., Zou, X., 2017. Anticancer activity of sesquiterpenoids extracted from *Solanum lyratum* via the induction of mitochondria-mediated apoptosis. Oncol Lett. 13 (1), 370–376.

Chevallier, A., 1996. The encyclopedia of medicinal plants: a practical reference guide to over 550 key herbs & their medicinal uses. Dorling Kindersley London, UK, 1996..

El Ashry, E., Rashed, N., Salama, O., Saleh, A., 2003. Components, therapeutic value and uses of myrrh. Die Pharmazie-An Int. J. Pharmaceut. Sci. 58, 163–168.

Francis, J.A., Raja, S.N., Nair, M.G., 2004. Bioactive terpenoids and guggulusteroids from *Commiphora mukul* gum resin of potential anti-inflammatory interest. Chem. Biodivers. 1, 1842–1853.

Lukas, B., Schmiderer, C., Franz, C., Novak, J., 2009. Composition of essential oil compounds from different Syrian populations of *Origanum syriacum* L. (Lamiaceae). J. Agric. Food Chem. 57, 1362–1365.

Massoud, A., El Sisi, S., Salama, O., 2001. Preliminary study of therapeutic efficacy of a new fasciolicidal drug derived from *Commiphora molmol* (myrrh). Am. J. Trop. Medi. Hyg. 65, 96–99.

Modzelewska, A., Sur, S., Kumar, S.K., Khan, S.R., 2005. Sesquiterpenes: natural products that decrease cancer growth. Curr. Med. Chem. Antican. Agents. 5 (5), 477–499.

Penuelas, J., Llusia, J., 1997. Effects of carbon dioxide, water supply, and seasonally on terpene content and emission by *Rosmarinus officinalis*. J. Chem. Ecol. 23, 979–993.

Rehman, M.T., AlAjmi, M.F., Hussein, A., Rather, G.M., Khan, M.A., 2019. High-throughput virtual screening and molecular dynamics simulation identified ZINC84525623 a potential inhibitor of NDM-1. Int. J. Mol. Sci. 20, 819.

Saadabi, A.M., Al-Sehemi, A., Al-Zailaie, K., 2006. In vitro antimicrobial activity of some Saudi Arabian plants used in folkloric medicine. Int. J. Bot. 2, 201–204.

Skehan, P., Storeng, R., Scudiero, D., Monks, A., McMahon, J., Vistica, D., Warren, J.T., Bokesch, H., Kenney, S., Boyd, M.R., 1990. New colorimetric cytotoxicity assay for anticancer-drug screening. J. Natl. Can. Inst. 82 (13), 1107–1112.

Stashenko, E.E., Martínez, J.R., Ruíz, C.A., Arias, G., Durán, C., Salgar, W., Cala, M., 2010. Lippia origanoides chemotype differentiation based on essential oil GC-MS and principal component analysis. J. Sep. Sci. 33, 93–103.

Velioglu, Y., Mazza, G., Gao, L., Oomah, B., 1998. Antioxidant activity and total phenolics in selected fruits, vegetables, and grain products. J. Agric. Food. Chem. 46, 4113–4117.